

Magneto-Optical Imaging of Transport Currents in $\text{YBa}_2\text{Cu}_3\text{O}_{7-x}$ on RABiTS™

D. Matthew Feldmann, Jodi L. Reeves, Anatolii A. Polyanskii, Amit Goyal, Ron Feenstra, D. F. Lee,
M. Paranthaman, D. M. Kroeger, D. K. Christen, Sue E. Babcock, David C. Larbalestier

Abstract—Two $\text{YBa}_2\text{Cu}_3\text{O}_{7-x}$ (YBCO) on RABiTS™ conductors with high $J_c(0 \text{ T}, 77 \text{ K})$ values of 2.3 and 2.4 MA/cm^2 were scribed by laser cutting to constrict supercurrent flow. On one of these tracks, magneto-optical (MO) imaging of the self-field produced by a transport current directly demonstrates the percolative nature of the current flow. Using Backscattered Electron Kikuchi Pattern (BEKP) analysis, we have found that Ni grain boundaries (GBs) $> 5^\circ$ generally introduce GBs in the YBCO that have lower J_c values than the intra-grain.

Index Terms—coated conductors, grain boundaries, magneto-optical imaging, RABiTS

I. INTRODUCTION

INDUSTRIAL applications of high-temperature superconducting wire or tape will require long lengths of conductors with a high critical current density (J_c) in large magnetic fields. One of the leading contenders of this technology is YBCO on RABiTS™. These conductors have already proven themselves on laboratory length scales [1], [2]. However even the best RABiTS™ samples have a significant number of GBs and possibly other defects with restrict the current carrying cross section and reduce J_c . From our previous work with textured Ni coated conductors (CCs) we found that all GBs $> 4^\circ$ had a critical current density which was less than the bulk (intra-grain) [3]. Since substrates cannot yet be textured to such a degree that no GBs greater than 4° are formed, it is important to understand what influence these higher angle GBs have on current flow.

Magneto-Optical imaging is most commonly done under the presence of magnetization currents alone [3]-[5]. Magnetization currents can be induced in a superconducting sample by applying a magnetic field. If a sufficiently strong magnetic field is applied the critical state can be induced everywhere in the sample, i.e. current flows at the *local* value of J_c everywhere. The electric field is near zero throughout the sample. Applying a potential difference across a sample induces transport currents. Generally the electric field is non-zero, and in an inhomogeneous sample, mathematical

modeling has shown that the electric field can be quite variable [6].

In this paper we combine MO imaging under both transport and magnetization currents with BEKP analysis to determine which GBs have reduced current densities relative to the bulk, and which GBs are most responsible for reduction of transport J_c .

II. EXPERIMENTAL

MO imaging, transport measurement, and BEKP analysis was performed on two high J_c coated conductors grown on RABiTS™. The architecture of both samples was YBCO/CeO₂/yttria-stabilized zirconia (YSZ)/CeO₂/Ni. A thickness of 300 nm for the YBCO layer and 500 nm for the buffer layers was determined by cross-sectional SEM. The YBCO was deposited by the BaF₂ method [7]. The full width of the samples was 3.4 mm with 4 mm between voltage taps. The $J_c(0 \text{ T}, 77 \text{ K})$ values at full width were 2.3 and 2.4 MA/cm^2 for the two samples at the $1\mu\text{V}/\text{cm}$ criterion. Smaller systems of GBs were later isolated by using a laser to cut tracks. The tracks were characterized by transport measurements in fields up to 1T and all reported J_c and I_c values are at the $1\mu\text{V}/\text{cm}$ criterion.

MO imaging was done at 40K and 77K under both magnetization and transport currents. The details of our standard imaging procedures are given elsewhere [4],[5]. Full voltage-current (VI) data was taken during the imaging of transport currents.

BEKP analysis was done on the Ni substrate after MO imaging and transport measurements. The YBCO was removed with a nitric acid etch and the buffer layers were removed by ion milling thereby exposing the underlying Ni substrate. Energy dispersive x-ray analysis confirmed that the buffer layers had been completely removed.

III. RESULTS AND DISCUSSION

Fig. 1(a) shows a MO image of the 2.3 MA/cm^2 sample before laser cutting. The magnetic flux penetration is clearly granular. This image is qualitatively similar to that found in our previous work [3], where it was shown that flux penetrates preferentially along GBs in the YBCO introduced by the Ni substrate. After MO imaging and transport measurements of the whole width, a track 1.8 mm x 265 μm was cut to limit supercurrent flow and isolate a smaller region of GBs for further study. This is shown schematically in Fig. 1(b). The average grain size of the Ni was $\sim 60 \mu\text{m}$ yielding a track $\sim 4-5$

Manuscript received September 16, 2000. This work was supported by the Air Force Office of Scientific Research Grant No. F49620-00-1-0091.

D. M. Feldmann, J. L. Reeves, A. A. Polyanskii, S. E. Babcock and D. C. Larbalestier are at the Applied Superconductivity Center, University of Wisconsin - Madison, Madison, WI 53706 USA (e-mail: feldmann@cae.wisc.edu)

A. Goyal, R. Feenstra, D. F. Lee, M. Paranthaman, D. M. Kroeger, and D. K. Christen are at Oak Ridge National Laboratory, Oak Ridge, TN 37831 (e-mail: f59@ornl.gov)

grains wide and ~ 30 grains, long. This track, hereafter referred to as track 1, had a $J_c(0 \text{ T}, 77 \text{ K})$ value of 0.7 MA/cm^2 , less than one-third the full width value. The $J_c(H)$ dependence was measured out to 1 T, and $J_c(1 \text{ T}, 77 \text{ K})$ was found to be 0.1 MA/cm^2 .

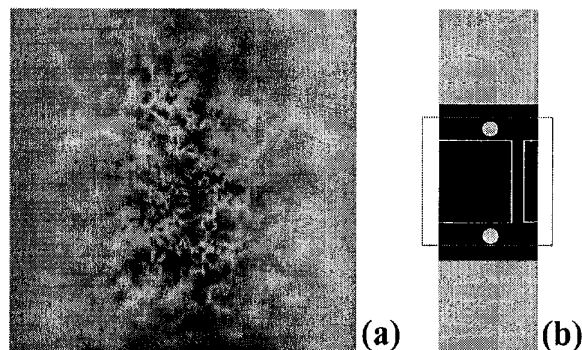


Fig. 1. Geometry and magneto-optical image. (a) Magneto-optical image across full width of sample, representative of both samples in the study. The sample was cooled in the absence of a field to 77K, and then a field of 80mT was applied. (b) Sample geometry. The black regions are YBCO and the gray areas are Ag. The thin white lines represent the track defined by laser cutting. The gray box shows the region of the MO image in (a).

Figs. 2(a) and (c) are MO images of magnetization currents flowing in track 1. For Fig. 2(a), the sample was zero field cooled (ZFC) to 77K, and then a field of 4.0 mT was applied. As the applied field increases, flux penetrates into the bulk from the track edges, but propagates preferentially along weaker linked regions such as some GBs. At 77 K, 4.0 mT was insufficient to induce the critical state in the track. At this low applied field only the weakest linked GBs appear in the MO image.

In Fig. 2(c) the sample has been ZFC to 40K, and then a field of 60 mT was applied. This was sufficient to induce the critical state in the track. From our previous work [4] we know that GBs appear in MO imaging when the critical current density of the GB (J_{cb}) is less than the critical current density of the bulk (J_{cg}). Using this information together with the knowledge that the track is in the critical state, we deduce that any GB *not* appearing in Fig. 2(c) is capable of carrying as much current as its *immediately surrounding grain*. Since MO imaging is sensitive to the ratio J_{cb}/J_{cg} , variations in the bulk J_c will also influence whether or not a given GB appears. It is expected that the bulk J_c in a RABiTS™ CC will be much more variable than in single crystal or bi-crystal substrates, as each Ni grain produces its own single crystal template for film growth. Variation in the vicinal angle of the grains and other factors may contribute to variable quality of the intra-grain.

Fig. 2(b) is a MO image of the self-field produced by transport currents in the track. The sample was ZFC to 77K, and then a current of 700 mA was applied. VI data was taken during MO imaging and I_c was found to be 560 mA. The MO image at an applied current of 560 mA was nearly identical to Fig. 2(b), but exhibited less contrast. It is immediately apparent that MO image under transport currents very closely resembles the image of magnetization currents, Fig. 2(a).

This reaffirms MO imaging under magnetization currents as a valid method of identifying *transport* current limiting defects, even though in the case of magnetization currents the electric field is near zero everywhere. The major current limiting obstacle in track 1 is the large GB cluster in the center of the track, between the markers **A** and **B** in Fig. 2(b). Notice that under transport current the flux penetration at the bottom of the GB cluster is increased relative to the rest of the cluster, unlike the Fig. 2(a). There is a clear gap in the flux between the GB cluster and the bottom edge of the track, and an increase in the magnetic flux at the track's bottom edge. This means that a large fraction of the current flowing in the track is being constricted and forced to flow between the GB cluster and the bottom edge of the track in the region **A-B**. In the region **B-C** of the track current flows mostly at the track edges, as predicted for a uniform superconducting thin strip [8],[9].

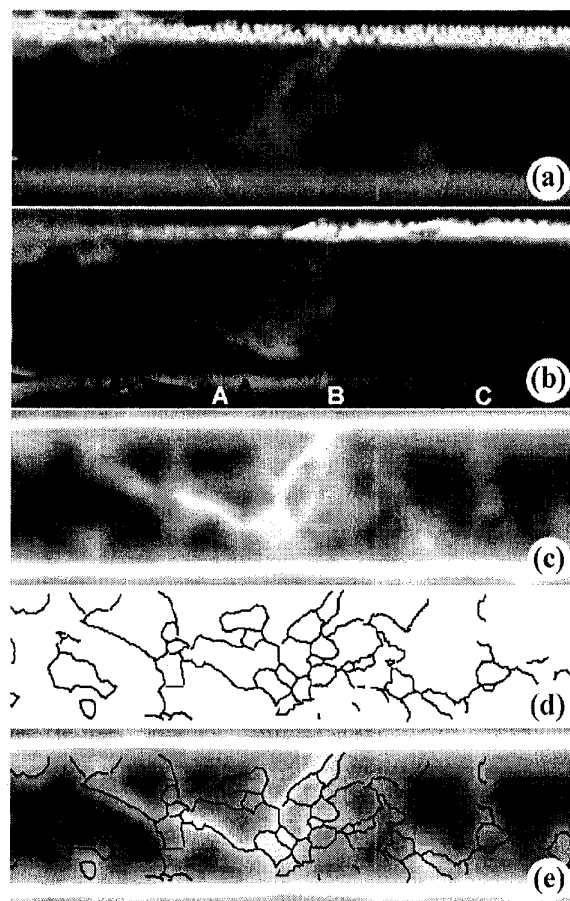


Fig. 2. MO images and EBKP data of track 1. Add a length marker to the image at bottom. (a) MO image of magnetization currents. Sample was zero field cooled (ZFC) to 77K, and then a field of 4.0 mT was applied. (b) MO image of self field. Sample was ZFC and then a transport current of 700 mA was applied. (c) MO image of magnetization currents. Sample was ZFC to 40K and then a field of 60 mT was applied. (d) GB map showing all boundaries $\geq 5^\circ$. This map matches well to the flux penetration of the Mo image in (d). (e) Overlay of (c) and (d).

In order to quantify the angles appearing in the MO

images, BEKP analysis was performed on the underlying Ni substrate. Fig. 2(d) is a map of all Ni GBs $\geq 5^\circ$. The overlay of Figs. 2(c) and (d), Fig. 2(e), shows that the $\geq 5^\circ$ GB map correlates well with the MO image. In fact, there is no flux penetration in Fig. 2(c) above Ni GBs less than 5° . While there is flux penetration above the majority of Ni GBs $\rho 5^\circ$, there is a small number of higher angle Ni GBs which do not appear in Fig. 2(c). This apparent inconsistency could be due to a variable J_{cb} in GBs with the same misorientation angle, a variable J_{cg} in the adjacent grains, or a difference in the actual GB angle in the YBCO relative to the Ni.

Threshold angles of 4° [3] and 5° degrees are rather high when judged against an exponential fall-off in J_c for increasing GB angle in [001] tilt bi-crystals [10], [11]. However, it should be considered that almost none of the GBs in track 1 are pure [001] tilt. The BEKP data shows almost equal numbers of GBs with rotation axes *near* [001], [011] and [111]. While the properties of [001] tilt YBCO GB have been extensively studied [10]-[13], little work has been done on low angle [011] or [111] GBs.

It is clear that there are far fewer GBs appearing in the MO image of transport currents than there are appearing in the MO image of the critical state, Fig. 2(c). For an applied transport current of 700 mA in Fig. 2(b), only GBs $\geq 7^\circ$ appear. This is not inconsistent with the results of the magnetization MO image. From the MO image of the critical state, we know that any GB not appearing has $J_{cb}/J_{cg} = 1$, and any boundary that is illuminated has $J_{cb}/J_{cg} < 1$. It might be expected that all GBs with $J_{cb}/J_{cg} < 1$ should appear under transport currents as well. However, at the applied current of 700 mA, the GBs $\geq 7^\circ$ have already driven the *whole* track to an electric field of $40 \mu\text{V}/\text{cm}$ before boundaries less than 7° begin to dissipate.

It deserves comment why the GB map of Fig. 2(d) was compared to a magnetization MO image at 40 K instead of 77 K. As temperature decreases, J_{cg} increases more rapidly than J_{cb} . Since MO imaging is measuring the ratio J_{cb}/J_{cg} , GBs are more clearly recognized at lower temperatures where the flux penetration into the bulk is relatively less. All the GBs visible in the critical state at 40K were also visible in the critical state at 77K.

A track was also cut on the second sample, track 2. At full width this sample had a $J_c(0 \text{ T}, 77 \text{ K})$ value of $2.4 \text{ MA}/\text{cm}^2$. Using the laser track 2 was cut $300 \mu\text{m}$ wide and 1.9 mm long. Voltage taps were placed at each end of the track and at the center. Both halves of track 2 had a $J_c(0 \text{ T}, 77 \text{ K})$ value of $0.6 \text{ MA}/\text{cm}^2$. MO imaging was then used to identify regions of apparent higher and lower J_c values. Once identified, the laser was again used to scribe smaller tracks directly over these regions of interest. The top one-third of the YBCO was removed by ion milling to reduce the effects of surface degradation on the numerical J_c values. Fig. 3(a) shows a MO image of a portion of track 2. It is unclear if J_{cg} , GBs, or the original width of the link² limited this value. The thin

white lines represent laser cuts that were made to isolate a region with relatively less structure in the MO image. This track had a $J_c(0 \text{ T}, 77 \text{ K})$ value of $2.7 \text{ MA}/\text{cm}^2$. Fig. 3(b) shows a second portion of the track where a bright cluster of GBs has been isolated by further laser cutting. This track had a $J_c(0 \text{ T}, 77 \text{ K})$ value of $1.7 \text{ MA}/\text{cm}^2$. Such a high J_c value may seem at odds with the MO image, but we emphasize that MO imaging is sensitive to the ratio J_{cb}/J_{cg} . The fact that the GB cluster of Fig. 3(b) appears quite bright in the MO image and has a high transport J_c values means that J_{cg} is likely much greater than both J_{cb} and the measured value of $1.7 \text{ MA}/\text{cm}^2$.

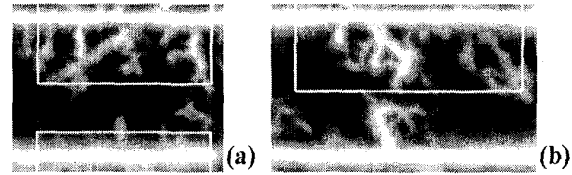


Fig. 3. MO images of portions of track 2. White lines denote where the laser was used to further restrict current flow. (a) The laser was used to scribe a track through a region which looked relatively well connected. (b) The laser was used to isolate a bright cluster of GBs.

BEKP analysis was performed on the two smaller tracks scribed into track 2. For both of the smaller tracks it was again found that only GBs $\geq 5^\circ$ appeared in the MO image.

IV. CONCLUSION

MO imaging of both magnetization and transport currents has been used to demonstrate the percolative nature of current flow in high J_c coated conductors. Good agreement of the two imaging modes is observed if one takes into account the different field configurations. Combined with BEKP analysis, we have shown that most GBs $\geq 5^\circ$ have a critical current that is less than the intra-grain J_{cg} . Conversely, it remains unclear lower GB misorientations whether the GBs limit J_c or the grains themselves. The threshold angles found here are not as sharp as those found previously [3], and there are a few Ni GBs $> 5^\circ$ which do not produce YBCO GBs that appear in the MO images. RABiTS™ type coated conductors can yield excellent J_c values, but the fact that many GBs remain obstacles to current flow even in the best samples indicates that there is room for the present technology to improve.

ACKNOWLEDGMENT

D.M.F. extends great thanks to G.A. Daniels for technical assistance.

² The original link was three times the width of the link in Fig. 3(a), and its J_c value is more than one-third less, $0.6 \text{ MA}/\text{cm}^2$. This value was

measured before ion milling, but the extent of the surface degradation was unknown.

REFERENCES

- [1] A. Goyal, S.X. Ren, E.D. Specht, D.M. Kroeger, R. Feenstra, D. Norton, M. Paranthaman, D.F. Lee, and D.K. Christen, *Micron*, vol. 30, pp. 563, 1999.
- [2] A. P. Malozemoff, S. Annavarapu, L. Fritzemeier, Q. Li, V. Prunier, M. Rupich, C. Thieme and W. Zhang, *Inst. of Phys. Conf. Series*, vol. 167, pp. 167, 2000.
- [3] D.M. Feldmann et al., "Influence of nickel substrate grain structure in on $\text{YBa}_2\text{Cu}_3\text{O}_{7-x}$ supercurrent connectivity in deformation-textured coated conductors," *Appl. Phys. Lett.*, vol. 77, pp. 2906, 2000.
- [4] A.A. Polyanskii et al., *Phys. Rev. B*, vol. 53, pp. 8687, 1996.
- [5] A.E. Pashitski et al., *Science*, vol. 275, pp. 367, 1997.
- [6] A. Gurevich and M. Friesen, *Phys Rev B*, vol. 62, pp. 4004, 2000.
- [7] R. Feenstra, T.B. Lindemer, J.B. Budai, and M.D. Galloway, *J. Appl. Phys.*, vol. 69, pp. 6569, 1991.
- [8] E.H. Brandt, M.V. Indenbom, A. Forkl, *Europhys. Lett.*, vol. 22, pp. 735, 1993.
- [9] E. Zeldov, J.R. Clem, M. McElfresh, M. Darwin, *Phys.Rev. B*, vol. 49, pp. 9802, 1994.
- [10] D. Dimos, P. Chaudhari, and J. Mannhart, *Phys. Rev. B*, vol. 41, pp. 4038, 1990.
- [11] D.T. Verebelyi et al., *Appl. Phys. Lett.*, vol. 76, pp. 1755, 2000.
- [12] N.F. Heinig, R.D. Redwing, J.E. Nordman, and D.C. Larbalestier, *Phys. Rev. B*, vol. 60, pp. 1409, 1999.
- [13] G.A. Daniels, A. Gurevich, and D.C. Larbalestier, *Appl. Phys. Lett.*, vol. 77, pp. 1, 2000.